Uniting Low- and High-Sensitivity Experiments through Generalised NMR Supersequences

Jonathan R. J. Yong,[1] Ēriks Kupče,[2] Tim D. W. Claridge[1,*]

[1] *Chemistry Research Laboratory, Department of Chemistry, University of Oxford, Mansfield Road, Oxford OX1 3TA, United Kingdom*

[2] *Bruker UK Ltd, R&D, Coventry CV4 9GH, United Kingdom*

[*] tim.claridge@chem.ox.ac.uk

---

https://www.rsc.org/journals-books-databases/about-journals/chemcomm#writing-guidelines

https://www.rsc.org/journals-books-databases/author-and-reviewer-hub/authors-information/prepare-and-format/

TODO: TOC graphic and TOC text (15–25 words)

Abstract

NOAH supersequences represent a time-efficient way of collecting multiple 2D NMR experiments. We show here that experiments with very different sensitivity requirements, including 1,1-ADEQUATE and HSQC, may be efficiently combined through interleaved supersequences, which assign each module a different number of transients and fully generalise the concept of parallel supersequences.

(50 words)

1 Introduction

Nuclear magnetic resonance (NMR) spectroscopy plays a key role in the structural elucidation of natural products; in particular, two-dimensional (2D) NMR experiments provide vast amounts of information on through-bond and through-space molecular connectivity.[1,2] However, these experiments are often time-consuming as they require the incrementation of indirect-dimension evolution periods in order to construct the requisite 2D data matrices. One particularly flexible method for accelerating 2D data acquisition is the NOAH (NMR by Ordered Acquisition using ^{1}H detection) technique,[3,4] in which multiple 2D experiments ('modules') are combined into a single experiment using only a single recovery delay. These nested 'supersequences', which rely on the tailored excitation of magnetisation from different isotopologues, provide an array of 2D spectra (up to 10 so far) in greatly reduced experiment times.

Virtually all common 2D experiments, such as HSQC, HMQC, COSY, TOCSY, and NOESY, have been exploited in NOAH supersequences, allowing for the (manual or computer-assisted) structural elucidation of a wide range of molecules.[5–7] However, such experiments tend to fall short in proton-sparse molecules[8–10] as they do not yield sufficient correlations. In such cases, additional information may be obtained through the HMBC[11–13] and HSQMBC[14–16] experiments which detect long-range X–^{1}H couplings ($^{n}J_{\mathrm{XH}}$, X = ^{13}C or ^{15}N). Although these tend to yield vastly more correlations, there often remains ambiguity in interpreting the resulting data as these techniques do not reveal the exact number of bonds over which a coupling is mediated. In contrast, one-bond ^{13}C–^{13}C correlations ($^{1}J_{\mathrm{CC}}$), obtained through the INADEQUATE[17]—or more practically, ADEQUATE[18,19]—experiments, allow chemists to directly trace out carbon- and nitrogen-containing backbones with much greater certainty. The main limitation of such experiments is their low sensitivity, as they rely on pairs of heteronuclei with low natural abundances; nonetheless, with the introduction of cryogenically cooled probes and concomitant advances in achievable signal-to-noise ratios (SNRs), such experiments can nowadays be feasibly run even on dilute samples.

To date, insensitive experiments such as ^{15}N HMBC and ADEQUATE have not been the main focus of NOAH supersequences.[20] This is because in a traditional 'linear' supersequence, each constituent module is recorded with the same number of transients. The total experiment duration is therefore dictated by the module with the lowest sensitivity, and higher-sensitivity modules (e.g. HSQC or COSY) would be recorded with far more transients than would be necessary. Although the more sensitive modules would still be obtained 'for free', the *effective* time savings thus realised would be far smaller than for a supersequence constructed from modules with balanced sensitivities.

For this reason, the low-sensitivity ADEQUATE and ^{15}N HMBC modules form a 'natural' pairing in the NOAH-2 AB$_{\mathrm{N}}$ supersequence introduced here (Figure 1b). However, in this work, we also go beyond the traditional 'linear' or 'horizontal' model of a supersequence in adding more modules through 'vertical' interleaving, in a similar fashion to the parallel supersequences recently described.[7] We show that, following an initial ADEQUATE module, up to four modules (^{15}N HMBC, ^{13}C HMBC, ^{15}N sensitivity-enhanced HSQC (seHSQC), and ^{13}C HSQC) may be interleaved in this 'vertical' fashion (Figures 1d and 1e), yielding five modules with balanced intensities and high-quality data. By tailoring the number of times each module is acquired, this technique provides a powerful and flexible way to balance modules with different sensitivities, and fully generalises our previous work on parallel supersequences, where only two modules were interleaved at a time.

2 NOAH-2 AB$_{\mathrm{N}}$

When designing NMR supersequences, it is generally a good rule of thumb to place the module with the lowest sensitivity first: this is because any incomplete preservation of magnetisation by earlier modules will lead to decreased sensitivity in later modules. The 1,1-ADEQUATE module, which relies on neighbouring pairs of ^{13}C nuclei—occurring only in roughly 1 out of 8130 molecules—therefore forms the beginning of all the supersequences described here.

The ADEQUATE module (Figure 1a) is designed to only use the magnetisation of protons directly bonded to ^{13}C, which we denote here as ^{1}H$^{\mathrm{C}}$.[22,23] In order to maintain the sensitivity of later modules, it must return

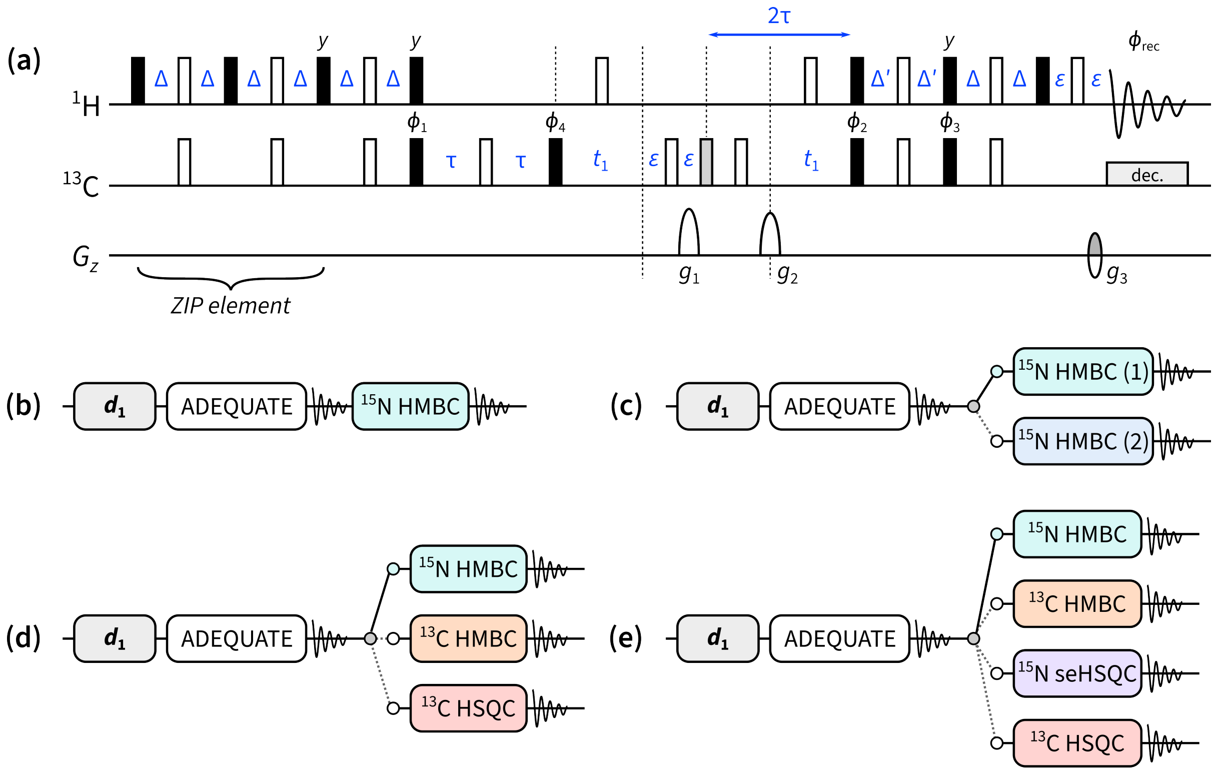

Figure 1: Pulse sequences described in this work. **(a)** ZIP-1,1-ADEQUATE module. Filled and empty bars refer to 90° and 180° pulses respectively; the grey filled bar is a 120° pulse for ^{13}C double-quantum to single-quantum coherence transfer.[21] Pulse and receiver phases are: $\phi_1 = x, -x$; $\phi_2 = 2\,(x), 2\,(-x)$; $\phi_3 = 2\,(y), 2\,(-y)$; $\phi_4 = 4\,(x), 4\,(-x)$; $\phi_{\text{rec}} = x, -x, -x, x, -x, x, x, -x$. Delays are set as follows: $\Delta = 1/(4 \cdot {}^1J_{\text{CH}})$, $\Delta' = 1/(8 \cdot {}^1J_{\text{CH}})$, and $\tau = 1/(4 \cdot {}^1J_{\text{CC}})$. ε is the minimum time required for a pulsed field gradient and the following recovery delay. Gradient amplitudes as a percentage of the maximum amplitude are: $g_1 = 78.5\%$, $g_2 = 77.6\%$, and $g_3 = -59\%$. Echo–antiecho selection is achieved by inverting the sign of g_3 as well as the pulse phase ϕ_3. **(b)** NOAH-2 AB_N supersequence. **(c)** NOAH-3 $\text{AB}_\text{N}\text{B}_\text{N}$, where the two ^{15}N HMBC experiments are optimised for two different values of $^nJ_{\text{NH}}$. **(d)** NOAH-4 $\text{AB}_\text{N}\text{BS}$. **(e)** NOAH-5 $\text{AB}_\text{N}\text{BS}_\text{N}^+\text{S}$.

the magnetisation of all other protons (denoted as $^1\text{H}^{!\text{C}}$) to the equilibrium $+z$ state. This is accomplished by replacing the initial 90° excitation pulse by the *zz* isotope-selective pulse element (ZIP),[23,24] which effects 90°_{-x} and 90°_{-y} rotations on $^1\text{H}^\text{C}$ and $^1\text{H}^{!\text{C}}$ magnetisation respectively. (Other isotope-specific elements such as BANGO[25–27] may also be used here, with similar results generally being obtained.[23]) The ^{15}N HMBC module of choice is a simple magnitude-mode version, with an optional first-order low-pass J-filter. In the NOAH-2 AB_N supersequence (ADEQUATE + ^{15}N HMBC, Figure 1b), this module simply consumes the remaining $^1\text{H}^{!\text{C}}$ magnetisation which was preserved by the ZIP-ADEQUATE module.

3 NOAH-3 $\text{AB}_\text{N}\text{B}_\text{N}$

Although this AB_N sequence performs well on its own (Figure 2), it suffers from the drawback that the ^{15}N HMBC is optimised for one specific value of $^nJ_{\text{NH}}$. In practice, $^nJ_{\text{NH}}$ values range from 2–16 Hz; in a

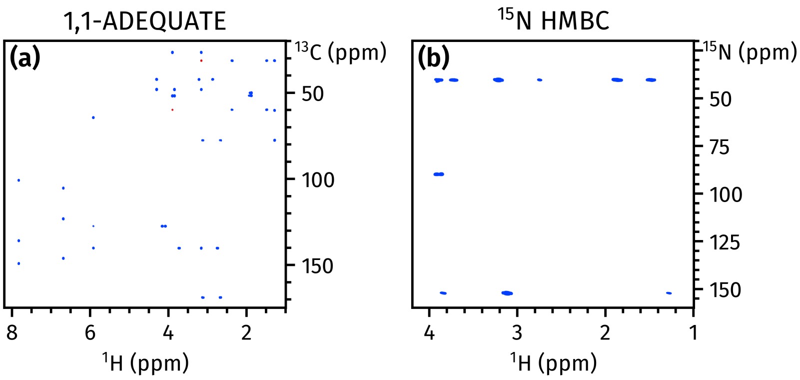

Figure 2: Spectra obtained from the NOAH-2 AB$_{\mathrm{N}}$ supersequence. **(a)** 1,1-ADEQUATE. **(b)** ^{15}N HMBC. Spectra were obtained on a 700 MHz Bruker AV III equipped with a TCI H/C/N cryoprobe; the sample used was 50 mᴍ brucine in $CDCl_3$.

single HMBC experiment, some correlations may therefore be lost due to J-coupling mismatch.

To circumvent this issue, a variety of accordion-type experiments[28–32] have been designed which decrement the J-evolution period in step with t_1, allowing a wider range of couplings to be sampled. Here, we adopt a different approach of recording two separate HMBC experiments optimised for different $^{n}J_{\mathrm{NH}}$ values, which in practice finds more common use. These two HMBC modules cannot be performed *sequentially*, as they both draw on the same ^{1}H$^{!\mathrm{C}}$ magnetisation; if concatenated 'horizontally' within a supersequence, the second HMBC would suffer from severely decreased sensitivity. However, they can easily be executed in an *interleaved* manner where, after the ADEQUATE module, the two HMBC experiments are alternately acquired.[7] In Figure 1c, this is illustrated by a 'vertical' stacking of the two modules. Thus, after each odd-numbered increment of the ADEQUATE, the first HMBC is acquired; and after each even-numbered increment, the second HMBC is acquired. This means that both HMBC spectra have half the usual number of t_1 increments compared to the ADEQUATE, which is acceptable since the ^{15}N dimension is typically sparse and a high resolution is not required. As can be seen in Figure 3, the two HMBC spectra reveal different sets of correlations.

4 NOAH-4 AB$_{\mathrm{N}}$BS

In the above AB$_{\mathrm{N}}$B$_{\mathrm{N}}$ experiment and in previous work,[7] we have shown how two alternating modules can be used to construct parallel supersequences. This concept can naturally be further generalised in order to allow $N \geq 2$ different experiments to be acquired alternately as the second module in the supersequence. These interleaved experiments can be arranged such that they each have lower resolution compared to the first module (as was done in the AB$_{\mathrm{N}}$B$_{\mathrm{N}}$ experiment), or such that they each have a fewer number of transients. In principle, such an arrangement can be used for *all* modules in a supersequence, not just the second module as is done here. However, it is important to remember that earlier modules affect the amount of magnetisation passed on to the later modules; thus, interleaving later modules in a sequence usually leads to more robust supersequences which do not have discrepancies in data intensity or spectral

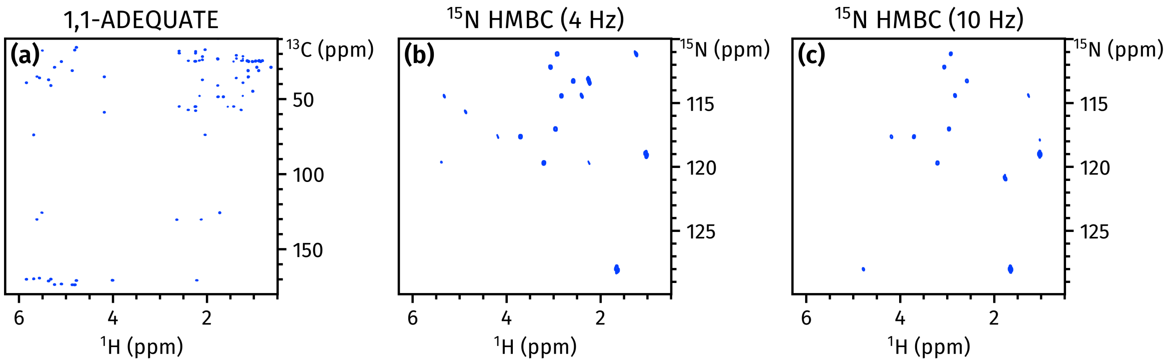

Figure 3: Spectra obtained from the NOAH-3 AB_NB_N supersequence. **(a)** 1,1-ADEQUATE (256 t_1 increments). **(b)** ^{15}N HMBC optimised for $^nJ_{NH} = 4$ Hz (128 t_1 increments). **(c)** ^{15}N HMBC optimised for $^nJ_{NH} = 10$ Hz (128 t_1 increments). Spectra were obtained on a 700 MHz Bruker AV III equipped with a TCI H/C/N cryoprobe; the sample used was 50 mM cyclosporin A in C_6D_6.

quality.

In the NOAH-4 AB_NBS supersequence (Figure 1d), the ADEQUATE module is followed by one of three choices: a ^{15}N HMBC, a ^{13}C HMBC, or a ^{13}C HSQC. Because these three latter modules do not have the same intrinsic sensitivity, we balance this by allocating a different number of transients to each module. In this specific example, each t_1 increment of the ADEQUATE is recorded a total of $8n$ times (where n is some positive integer); the ^{15}N HMBC $6n$ times; and the ^{13}C HMBC and HSQC n times each. The value of n is chosen to ensure that all spectra have sufficient sensitivity; the spectra in Figure 4 were acquired with $n = 2$. Using the pulse programmes provided in the *Supplementary Information*, the exact number of transients for each module can be customised via user-defined constants. The exact implementation of these supersequences is described further in Section S1.

One additional feature of the supersequence above concerns the fact that the ^{13}C HSQC module is placed immediately after the ADEQUATE. Both of these modules draw on the same $^1H^C$ magnetisation pool, and this generally causes the latter module (here HSQC) to suffer from sensitivity losses. Since the HSQC has a much greater intrinsic sensitivity compared to the ADEQUATE, this loss would in fact be tolerable. However, in this experiment, we chose to add a period of isotropic DIPSI-2 mixing[33] immediately before the HSQC module to effect $^1H^{!C} \rightarrow {}^1H^C$ magnetisation transfer, as has previously been done in ASAP[34–37] and NOAH[23] experiments: this replenishes some of the lost $^1H^C$ magnetisation and leads to greater intensities for the HSQC (Figure S3). This mixing period does not need to be inserted prior to either of the ^{15}N or ^{13}C HMBC modules, as they do not use $^1H^C$ magnetisation.

The acquisition of the NOAH-4 AB_NBS spectra in Figure 4 took 124 minutes; in contrast, normal acquisition of all four experiments (with the appropriate number of transients) required a total of 223 minutes. As the ADEQUATE is placed first in the supersequence, its sensitivity is almost identical to that of a standalone ADEQUATE; the inclusion of the ZIP element causes only an approximate 5% loss. The ^{15}N and ^{13}C HMBC spectra experience small losses (16–29%) in sensitivity, due to imperfect magnetisation

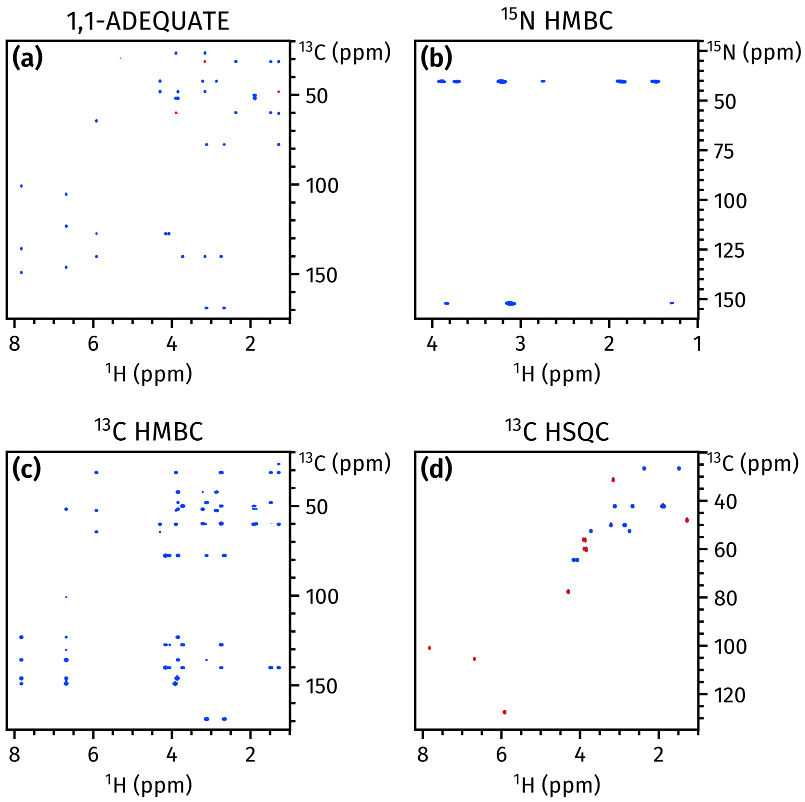

Figure 4: Spectra obtained from the NOAH-4 AB_NBS supersequence. **(a)** 1,1-ADEQUATE (16 transients). **(b)** ^{15}N HMBC (12 transients). **(c)** ^{13}C HMBC (2 transients). **(d)** ^{13}C HSQC (2 transients). Spectra were obtained on a 700 MHz Bruker AV III equipped with a TCI H/C/N cryoprobe; the sample used was 50 mM brucine in $CDCl_3$.

retention by the ADEQUATE module. This is, however, outweighed by the almost twofold time savings provided by concatenation of the modules: if the NOAH supersequence were acquired for as long as the standalone experiments were, the ^{15}N HMBC spectra would have almost the same SNR, and the ^{13}C HMBC from the NOAH would in fact have a 12% improvement in SNR. Due to the reuse of $^{1}H^{C}$ magnetisation, the HSQC module only retains 29% of its original sensitivity. However, as the HSQC is still two orders of magnitude more sensitive than the ADEQUATE, this decrease is readily tolerated; if necessary, the sensitivity-enhanced HSQC module[23,24,38,39] may also be used in its place.

While this combination of modules proves to be particularly elegant in that it furnishes virtually all heteronuclear correlations needed for structural assignment, it is by no means the only valid one. The principle of interleaved modules can be used to incorporate almost any experiment that may be required: as an example, spectra from a NOAH-4 AB_NNS experiment (N = NOESY, which replaces the ^{13}C HMBC) are shown in Figure S2.

5 NOAH-5 $AB_NBS_N^+S$

As a final example, we add a further ^{15}N seHSQC module to the above sequence. The ^{15}N seHSQC uses only ^{1}H^{N} magnetisation (i.e. protons directly bonded to ^{15}N), which is separate from all other modules introduced so far. Thus, in principle, it can simply be added *linearly* as a third module to the supersequence: such an arrangement would maximise its sensitivity as the ^{15}N seHSQC data is collected on every scan in the supersequence. Such an arrangement would, however, compromise the performance of the other modules, as they must then be modified to preserve the requisite ^{1}H^{N} magnetisation: for example, the HMBC modules would need to be modified to include the *zz*-filter,[5,6] which generally causes 10–20% sensitivity losses. Instead of this, the ^{15}N seHSQC can most efficiently be implemented in a 'vertical', interleaved manner, by simply reducing the number of transients for the ^{15}N HMBC by *n* and diverting these towards the ^{15}N seHSQC. This means that the second slot in the supersequence now alternates between four different experiments, as shown in Figure 1e. This example especially illustrates how the use of interleaved *and* sequential acquisition leads to much greater flexibility in supersequence design, especially when considering the relative sensitivities of different modules.

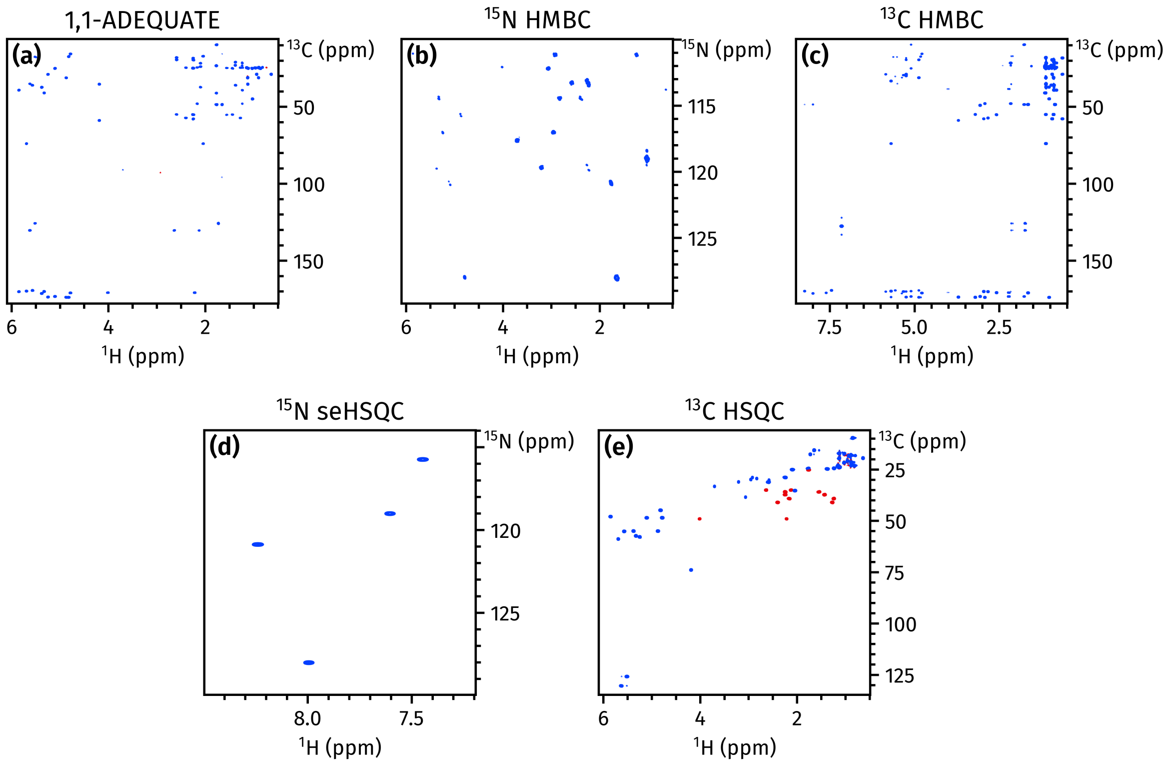

Figure 5: Spectra obtained from the NOAH-5 $AB_NBS_N^+S$ supersequence. **(a)** 1,1-ADEQUATE (16 transients). **(b)** ^{15}N HMBC (10 transients). **(c)** ^{13}C HMBC (2 transients). **(d)** ^{15}N sensitivity-enhanced HSQC (2 transients). **(e)** ^{13}C HSQC (2 transients). Spectra were obtained on a 700 MHz Bruker AV III equipped with a TCI H/C/N cryoprobe; the sample used was 50 mM cyclosporin A in C_6D_6.

The five spectra obtained from this sequence are shown in Figure 5. Collectively, this supersequence provides virtually all heteronuclear correlation data required for structural elucidation or assignment. This is similar in spirit to the PANACEA experiment,[40,41] but yields greater sensitivity as it uses equilibrium ^{1}H magnetisation rather than the low-magnetogyric ratio ^{13}C and ^{15}N nuclei, and does not require multiple-receiver hardware.[4,42] Of course, the ADEQUATE experiment may not be necessary for every novel compound encountered; however, in cases where it *is* needed, the supersequences described here demonstrate that other valuable heteronuclear spectra can also be acquired in a time-efficient manner along with the ADEQUATE.

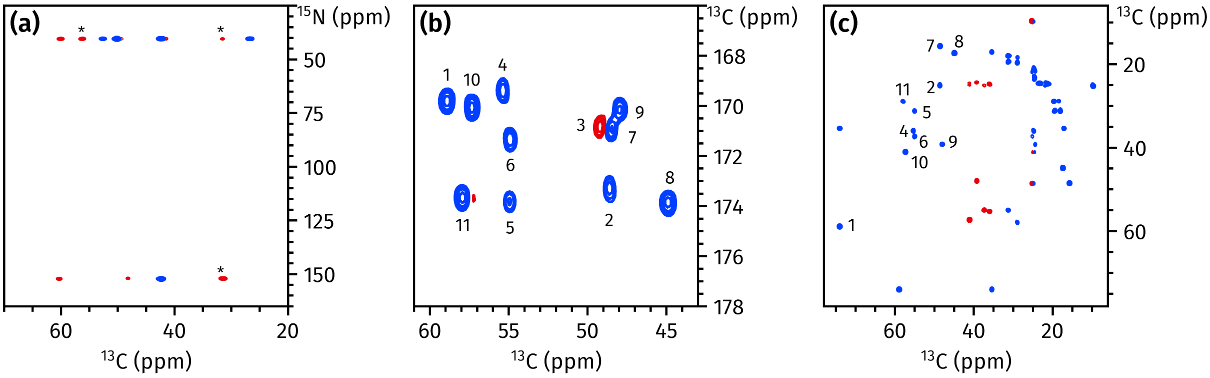

Figure 6: Spectra obtained through indirect covariance processing. In all cases the peak sign indicates carbon multiplicity; this information is contained in the multiplicity-edited ^{13}C HSQC spectrum and arises naturally during covariance processing. **(a)** ^{13}C–^{15}N correlation spectrum (containing both one- and multiple-bond correlations) obtained by processing the brucine ^{15}N HMBC and ^{13}C HSQC spectra (in Figures 4b and 4d) using unsymmetric indirect covariance. Some artefacts (arising from peak overlap in the ^{1}H dimension) are marked with asterisks. **(b–c)** Insets of ^{13}C–^{13}C one-bond correlation spectrum, obtained by processing the cyclosporin ADEQUATE and ^{13}C HSQC spectra (in Figures 5a and 5e) using generalised indirect covariance ($\lambda = 0.5$). The Cα–CO correlations, numbered by residue (see Figure S4), are shown in (b). Sidechain C−C correlations are shown in (c); only peaks corresponding to Cα–Cβ correlations are labelled. The inset in (c) has been further subjected to a sign-preserving symmetrisation procedure, described further in Section S5.

Furthermore, the heteronuclear spectra collected this way can be processed using indirect covariance processing[43–45] to yield other forms of correlation spectra. For example, the ^{15}N HMBC and ^{13}C HSQC can be used to generate ^{13}C–^{15}N correlation spectra.[46–48] Furthermore, the ^{13}C HSQC and ADEQUATE experiments can be used to create ^{13}C–^{13}C one-bond correlation spectra.[49,50] It should be further emphasised that all of the 'base' spectra used as the inputs here are obtained *in a single measurement* using either the NOAH-4 or NOAH-5 supersequences discussed above. A notable benefit of this is that t_1 for all modules are incremented simultaneously: this minimises the effects of temporal variations such as temperature drift or chemical reactions, which can lead to inaccurate peaks in covariance spectra.

6 Conclusion(ish)

In conclusion, we have demonstrated here how low-sensitivity experiments, such as 1,1-ADEQUATE and ^{15}N HMBC, may be optimally combined in NMR supersequences, leading to substantial reductions in experiment time. Through a generalisation of our previous concept of parallel supersequences, further high-sensitivity modules may be added to the supersequence both 'horizontally' and 'vertically', corresponding respectively to sequential and interleaved acquisition. The spectra thus obtained provide the chemist with far more powerful tools for the characterisation of complex molecules, especially in cases where existing NOAH supersequences do not provide sufficient information for unambiguous assignment.

While the generalised supersequences presented here enable modules to be assembled in almost any imaginable way, their increasing complexity mean that pulse programme construction is more difficult. At present, the GENESIS tool for automatic pulse sequence generation[51] provides only limited options for parallel supersequences. In particular, it is restricted to only *two* different interleaved modules (as demonstrated in previous work[7]). Thus, the pulse programmes used in this work were constructed by hand. On top of this, new AU programmes are also required to process the data correctly. The pulse sequences and processing scripts used in this work are provided in the Bruker User Library, accessible at `https://www.bruker.com/en/services/bruker-user-library.html`.

Acknowledgements

We thank Dr Mohammadali Foroozandeh (University of Oxford) for helpful discussions. J.R.J.Y. thanks the Clarendon Fund (University of Oxford) and the EPSRC Centre for Doctoral Training in Synthesis for Biology and Medicine (EP/L015838/1) for a studentship, generously supported by AstraZeneca, Diamond Light Source, Defence Science and Technology Laboratory, Evotec, GlaxoSmithKline, Janssen, Novartis, Pfizer, Syngenta, Takeda, UCB, and Vertex.

References

(1) Findeisen, M.; Berger, S., *50 and More Essential NMR Experiments: A Detailed Guide*; Wiley: Weinheim, 2013.

(2) Claridge, T. D. W., *High-Resolution NMR Techniques in Organic Chemistry*, 3rd ed.; Elsevier: Amsterdam, 2016.

(3) Kupče, Ē.; Claridge, T. D. W. NOAH: NMR Supersequences for Small Molecule Analysis and Structure Elucidation. *Angew. Chem., Int. Ed.* **2017**, *56*, 11779–11783, DOI: `10.1002/anie.201705506`.

(4) Kupče, Ē.; Frydman, L.; Webb, A. G.; Yong, J. R. J.; Claridge, T. D. W. Parallel nuclear magnetic resonance spectroscopy. *Nat. Rev. Methods Primers* **2021**, *1*, 27, DOI: `10.1038/s43586-021-00024-3`.

(5) Kupče, Ē.; Claridge, T. D. W. Molecular structure from a single NMR supersequence. *Chem. Commun.* **2018**, *54*, 7139–7142, DOI: `10.1039/c8cc03296c`.

(6) Kupče, Ē.; Claridge, T. D. W. New NOAH modules for structure elucidation at natural isotopic abundance. *J. Magn. Reson.* **2019**, *307*, 106568, DOI: `10.1016/j.jmr.2019.106568`.

(7) Kupče, Ē.; Yong, J. R. J.; Widmalm, G.; Claridge, T. D. W. Parallel NMR Supersequences: Ten Spectra in a Single Measurement. *JACS Au* **2021**, DOI: 10.1021/jacsau.1c00423.

(8) White, K. N.; Amagata, T.; Oliver, A. G.; Tenney, K.; Wenzel, P. J.; Crews, P. Structure Revision of Spiroleucettadine, a Sponge Alkaloid with a Bicyclic Core Meager in H-Atoms. *J. Org. Chem.* **2008**, *73*, 8719–8722, DOI: 10.1021/jo800960w.

(9) Senior, M. M.; Williamson, R. T.; Martin, G. E. Using HMBC and ADEQUATE NMR Data To Define and Differentiate Long-Range Coupling Pathways: Is the Crews Rule Obsolete? *J. Nat. Prod.* **2013**, *76*, 2088–2093, DOI: 10.1021/np400562u.

(10) Buevich, A. V.; Williamson, R. T.; Martin, G. E. NMR Structure Elucidation of Small Organic Molecules and Natural Products: Choosing ADEQUATE vs HMBC. *J. Nat. Prod.* **2014**, *77*, 1942–1947, DOI: 10.1021/np500445s.

(11) Bax, A.; Summers, M. F. Proton and carbon-13 assignments from sensitivity-enhanced detection of heteronuclear multiple-bond connectivity by 2D multiple quantum NMR. *J. Am. Chem. Soc.* **1986**, *108*, 2093–2094, DOI: 10.1021/ja00268a061.

(12) Crouch, R. C.; Llanos, W.; Mehr, K. G.; Hadden, C. E.; Russell, D. J.; Martin, G. E. Applications of cryogenic NMR probe technology to long-range ^{1}H–^{15}N 2D NMR studies at natural abundance. *Magn. Reson. Chem.* **2001**, *39*, 555–558, DOI: 10.1002/mrc.886.

(13) Martin, G. E.; Williams, A. J. Applications of ^{1}H–^{15}N Long-Range Heteronuclear Shift Correlation and ^{15}N NMR in Alkaloid Chemistry. *Annu. Rep. NMR Spectrosc.* **2015**, *84*, 1–76, DOI: 10.1016/bs.arnmr.2014.10.003.

(14) Williamson, R. T.; Buevich, A. V.; Martin, G. E.; Parella, T. LR-HSQMBC: A Sensitive NMR Technique To Probe Very Long-Range Heteronuclear Coupling Pathways. *J. Org. Chem.* **2014**, *79*, 3887–3894, DOI: 10.1021/jo500333u.

(15) Castañar, L.; Saurí, J.; Williamson, R. T.; Virgili, A.; Parella, T. Pure In-Phase Heteronuclear Correlation NMR Experiments. *Angew. Chem., Int. Ed.* **2014**, *53*, 8379–8382, DOI: 10.1002/anie.201404136.

(16) Saurí, J.; Liu, Y.; Parella, T.; Williamson, R. T.; Martin, G. E. Selecting the Most Appropriate NMR Experiment to Access Weak and/or Very Long-Range Heteronuclear Correlations. *J. Nat. Prod.* **2016**, *79*, 1400–1406, DOI: 10.1021/acs.jnatprod.6b00139.

(17) Bax, A.; Freeman, R.; Frenkiel, T. A. An NMR technique for tracing out the carbon skeleton of an organic molecule. *J. Am. Chem. Soc.* **1981**, *103*, 2102–2104, DOI: 10.1021/ja00398a044.

(18) Reif, B.; Köck, M.; Kerssebaum, R.; Kang, H.; Fenical, W.; Griesinger, C. ADEQUATE, a New Set of Experiments to Determine the Constitution of Small Molecules at Natural Abundance. *J. Magn. Reson., Ser. A* **1996**, *118*, 282–285, DOI: 10.1006/jmra.1996.0038.

(19) Martin, G. E. Using 1,1- and 1,*n*-ADEQUATE 2D NMR Data in Structure Elucidation Protocols. *Annu. Rep. NMR Spectrosc.* **2011**, *74*, 215–291, DOI: 10.1016/B978-0-08-097072-1.00005-4.

(20) Rao Kakita, V. M.; Hosur, R. V. All-in-one NMR spectroscopy of small organic molecules: complete chemical shift assignment from a single NMR experiment. *RSC Adv.* **2020**, *10*, 21174–21179, DOI: 10.1039/d0ra03417g.

(21) Mareci, T. H.; Freeman, R. Echoes and antiechoes in coherence transfer NMR: Determining the signs of double-quantum frequencies. *J. Magn. Reson.* **1982**, *48*, 158–163, DOI: 10.1016/0022-2364(82)90250-5.

(22) Orts, J.; Gossert, A. D. Structure determination of protein-ligand complexes by NMR in solution. *Methods* **2018**, *138-139*, 3–25, DOI: 10.1016/j.ymeth.2018.01.019.

(23) Yong, J. R. J.; Hansen, A. L.; Kupče, Ē.; Claridge, T. D. W. Increasing sensitivity and versatility in NMR supersequences with new HSQC-based modules. *J. Magn. Reson.* **2021**, *329*, 107027, DOI: 10.1016/j.jmr.2021.107027.

(24) Hansen, A. L.; Kupče, Ē.; Li, D.-W.; Bruschweiler-Li, L.; Wang, C.; Brüschweiler, R. 2D NMR-Based Metabolomics with HSQC/TOCSY NOAH Supersequences. *Anal. Chem.* **2021**, *93*, 6112–6119, DOI: 10.1021/acs.analchem.0c05205.

(25) Sørensen, O. W. Selective Rotations Using Non-Selective Pulses and Heteronuclear Couplings. *Bull. Magn. Reson.* **1994**, *16*, 49–53.

(26) Nagy, T. M.; Gyöngyösi, T.; Kövér, K. E.; Sørensen, O. W. BANGO SEA XLOC/HMBC–H2OBC: complete heteronuclear correlation within minutes from one NMR pulse sequence. *Chem. Commun.* **2019**, *55*, 12208–12211, DOI: 10.1039/c9cc06253j.

(27) Nagy, T. M.; Kövér, K. E.; Sørensen, O. W. NORD: NO Relaxation Delay NMR Spectroscopy. *Angew. Chem., Int. Ed.* **2021**, *60*, 13587–13590, DOI: 10.1002/anie.202102487.

(28) Wagner, R.; Berger, S. ACCORD-HMBC: a superior technique for structural elucidation. *Magn. Reson. Chem.* **1998**, *36*, S44–S46, DOI: 10.1002/(sici)1097-458x(199806)36:13<s44::aid-omr281>3.0.co;2-q.

(29) Martin, G. E.; Hadden, C. E.; Crouch, R. C.; Krishnamurthy, V. V. ACCORD-HMBC: advantages and disadvantages of static versus accordion excitation. *Magn. Reson. Chem.* **1999**, *37*, 517–528, DOI: 10.1002/(sici)1097-458x(199908)37:8<517::aid-mrc501>3.0.co;2-w.

(30) Hadden, C. E.; Martin, G. E.; Krishnamurthy, V. V. Improved Performance Accordion Heteronuclear Multiple-Bond Correlation Spectroscopy—IMPEACH-MBC. *J. Magn. Reson.* **1999**, *140*, 274–280, DOI: 10.1006/jmre.1999.1840.

(31) Martin, G. E.; Hadden, C. E. Application of accordion excitation in ^{1}H–^{15}N long-range heteronuclear shift correlation experiments at natural abundance. *Magn. Reson. Chem.* **2000**, *38*, 251–256, DOI: 10.1002/(sici)1097-458x(200004)38:4<251::aid-mrc625>3.0.co;2-j.

(32) Hadden, C. E.; Martin, G. E.; Krishnamurthy, V. V. Constant time inverse-detection gradient accordion rescaled heteronuclear multiple bond correlation spectroscopy: CIGAR-HMBC. *Magn. Reson. Chem.* **2000**, *38*, 143–147, DOI: 10.1002/(sici)1097-458x(200002)38:2<143::aid-mrc624>3.0.co;2-s.

(33) Shaka, A. J.; Lee, C. J.; Pines, A. Iterative schemes for bilinear operators; application to spin decoupling. *J. Magn. Reson.* **1988**, *77*, 274–293, DOI: 10.1016/0022-2364(88)90178-3.

(34) Schulze-Sünninghausen, D.; Becker, J.; Luy, B. Rapid Heteronuclear Single Quantum Correlation NMR Spectra at Natural Abundance. *J. Am. Chem. Soc.* **2014**, *136*, 1242–1245, DOI: 10.1021/ja411588d.

(35) Schulze-Sünninghausen, D.; Becker, J.; Koos, M. R. M.; Luy, B. Improvements, extensions, and practical aspects of rapid ASAP-HSQC and ALSOFAST-HSQC pulse sequences for studying small molecules at natural abundance. *J. Magn. Reson.* **2017**, *281*, 151–161, DOI: 10.1016/j.jmr.2017.05.012.

(36) Koos, M. R. M.; Luy, B. Polarization recovery during ASAP and SOFAST/ALSOFAST-type experiments. *J. Magn. Reson.* **2019**, *300*, 61–75, DOI: 10.1016/j.jmr.2018.12.014.

(37) Becker, J.; Koos, M. R. M.; Schulze-Sünninghausen, D.; Luy, B. ASAP-HSQC-TOCSY for fast spin system identification and extraction of long-range couplings. *J. Magn. Reson.* **2019**, *300*, 76–83, DOI: 10.1016/j.jmr.2018.12.021.

(38) Palmer, A. G.; Cavanagh, J.; Wright, P. E.; Rance, M. Sensitivity improvement in proton-detected two-dimensional heteronuclear correlation NMR spectroscopy. *J. Magn. Reson.* **1991**, *93*, 151–170, DOI: 10.1016/0022-2364(91)90036-S.

(39) Kay, L.; Keifer, P.; Saarinen, T. Pure absorption gradient enhanced heteronuclear single quantum correlation spectroscopy with improved sensitivity. *J. Am. Chem. Soc.* **1992**, *114*, 10663–10665, DOI: 10.1021/ja00052a088.

(40) Kupče, Ē.; Freeman, R. Molecular Structure from a Single NMR Experiment. *J. Am. Chem. Soc.* **2008**, *130*, 10788–10792, DOI: 10.1021/ja8036492.

(41) Kupče, Ē.; Freeman, R. Molecular structure from a single NMR sequence (fast-PANACEA). *J. Magn. Reson.* **2010**, *206*, 147–153, DOI: 10.1016/j.jmr.2010.06.018.

(42) Kupče, Ē.; Mote, K. R.; Webb, A.; Madhu, P. K.; Claridge, T. D. W. Multiplexing experiments in NMR and multi-nuclear MRI. *Prog. Nucl. Magn. Reson. Spectrosc.* **2021**, *124-125*, 1–56, DOI: 10.1016/j.pnmrs.2021.03.001.

(43) Zhang, F.; Brüschweiler, R. Indirect Covariance NMR Spectroscopy. *J. Am. Chem. Soc.* **2004**, *126*, 13180–13181, DOI: 10.1021/ja047241h.

(44) Snyder, D. A.; Brüschweiler, R. Generalized Indirect Covariance NMR Formalism for Establishment of Multidimensional Spin Correlations. *J. Phys. Chem. A* **2009**, *113*, 12898–12903, DOI: 10.1021/jp9070168.

(45) Jaeger, M.; Aspers, R. L. E. G. Covariance NMR and Small Molecule Applications. *Annu. Rep. NMR Spectrosc.* **2014**, *83*, 271–349, DOI: 10.1016/B978-0-12-800183-7.00005-8.

(46) Kupče, E.; Freeman, R. Natural-abundance ^{15}N–^{13}C correlation spectra of vitamin B-12. *Magn. Reson. Chem.* **2007**, *45*, 103–105, DOI: 10.1002/mrc.1947.

(47) Martin, G. E.; Hilton, B. D.; Irish, P. A.; Blinov, K. A.; Williams, A. J. ^{13}C–^{15}N connectivity networks via unsymmetrical indirect covariance processing of ^{1}H–^{13}C HSQC and ^{1}H–^{15}N IMPEACH spectra. *Journal of Heterocyclic Chemistry* **2007**, *44*, 1219–1222, DOI: 10.1002/jhet.5570440541.

(48) Martin, G. E.; Irish, P. A.; Hilton, B. D.; Blinov, K. A.; Williams, A. J. Utilizing unsymmetrical indirect covariance processing to define ^{15}N–^{13}C connectivity networks. *Magn. Reson. Chem.* **2007**, *45*, 624–627, DOI: 10.1002/mrc.2029.

(49) Martin, G. E.; Hilton, B. D.; Blinov, K. A. HSQC-ADEQUATE correlation: a new paradigm for establishing a molecular skeleton. *Magn. Reson. Chem.* **2011**, *49*, 248–252, DOI: 10.1002/mrc.2743.

(50) Martin, G. E.; Hilton, B. D.; Willcott III, M. R.; Blinov, K. A. HSQC-ADEQUATE: an investigation of data requirements. *Magn. Reson. Chem.* **2011**, *49*, 350–357, DOI: 10.1002/mrc.2757.

(51) Yong, J. R. J.; Kupče, Ē.; Claridge, T. D. W. Modular Pulse Program Generation for NMR Supersequences. *Anal. Chem.* **2022**, *94*, 2271–2278, DOI: 10.1021/acs.analchem.1c04964.

Supporting Information

for

Uniting Low- and High-Sensitivity Experiments through Generalised NMR Supersequences

Jonathan R. J. Yong,[1] Ēriks Kupče,[2] Tim D. W. Claridge[1,*]

[1] *Chemistry Research Laboratory, Department of Chemistry, University of Oxford, Mansfield Road, Oxford OX1 3TA, United Kingdom*

[2] *Bruker UK Ltd, R&D, Coventry CV4 9GH, United Kingdom*

[*] tim.claridge@chem.ox.ac.uk

Contents

S1 Pulse programme description

This section presents a more detailed description of how the pulse programme works; this information is important to anybody seeking to use the pulse programmes given here (or anybody writing similar 'interleaved' experiments). We use the NOAH-4 AB_NBS experiment as an example here. In this experiment, the second module alternates between the ^{15}N HMBC (B_N), ^{13}C HMBC (B), and ^{13}C HSQC (S); the pulse programme is set up such that these three modules have fewer transients than the ADEQUATE (A). For every 8 transients of the ADEQUATE, 6, 1, and 1 transient(s) are recorded respectively for the B_N, B, and S modules.

Generally, interleaving is performed using modular arithmetic. A loop counter (L3) is used in order to keep track of how many transients have been recorded so far, and the value of this counter *modulo* 8 is used in order to determine which module to run in the second slot. Note that this is independent of the NS parameter in TopSpin. So, each t_1 increment of the ADEQUATE module is actually recorded 8 × NS times.

```
  "l3 = 0"      ; initialise loop counter
  "cnst51 = 8"  ; number of transients for ADEQUATE
  "cnst52 = 6"  ; number of transients for 15N HMBC
  "cnst53 = 1"  ; number of transients for 13C HMBC
2 d1
  ; run ADEQUATE
  goscnp ph30   ; record ADEQUATE FID
  if "l3 % cnst51 < cnst52" {
    ; transients 1 through 6, run 15N HMBC
    go=2 ph31
  }
  else {
  if "l3 % cnst51 < cnst52 + cnst53" {
    ; transient 7, run 13C HMBC
    go=2 ph31
  }
  else {
    ; transient 8, run 13C HSQC
    go=2 ph31   ; 'go' loops back to the label '2' a total of NS times
  }
  }
  1m iu3   ; increment loop counter
  ; increment t1 here and proceed
```

Of course, the values of cnst51, cnst52, and cnst53 are not hardcoded as in the example above. By changing these numbers, the user can control the number of transients allocated to each module. In total, each t_1 increment of the ADEQUATE module is acquired cnst51 × NS times; the ^{15}N HMBC is acquired cnst52 × NS times; and so on. (For the final module (HSQC), there is no need to define an analogous cnst54 because it simply 'uses up' all the remaining transients; thus, the HSQC is acquired a total of (cnst51 − cnst52 − cnst53) × NS times.)

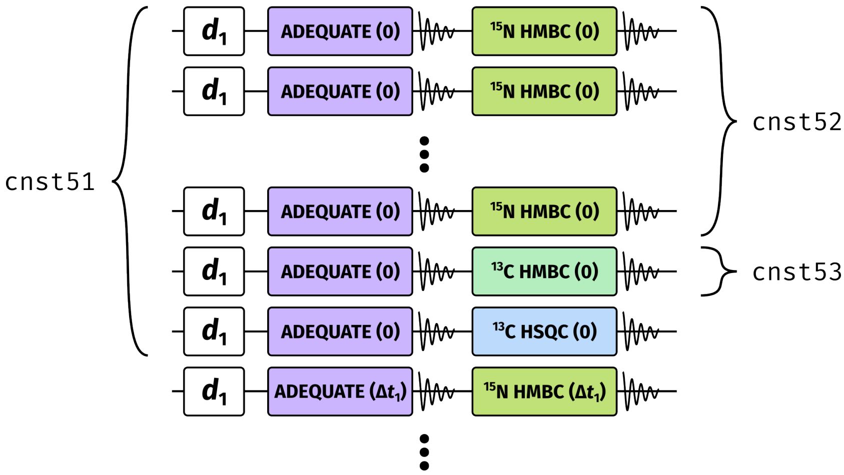

Figure S1: Diagram illustrating the practical implementation of the NOAH-4 AB$_N$BS supersequence. Numbers in parentheses refer to the value of t_1; the first increment is recorded with $t_1 = 0$ for all modules. d_1 represents a recovery delay. Each row is repeated NS times, during which phase cycling is performed; however, no phase cycling is performed *between* rows, even those which are identical (e.g. the first two rows). Since each row only consists of two horizontally concatenated modules, the NBL parameter is to be still set to 2.

It is worth pointing out at this point that, because of the way TopSpin increments pulse phase pointers, *phase cycling* (as defined by the phase tables in the pulse programme) is only carried out NS times. That is, although the ADEQUATE module is recorded cnst51 × NS times, only a NS-step phase cycle is being used. With modern gradient-based coherence selection techniques, this does not have a substantial impact on the data quality. (For example, the data in Figure 4 were recorded with NS=2 and are perfectly serviceable.) Nevertheless, it is always a good idea to make NS as large as possible, and always at least 2 to ensure suppression of axial peaks. As a concrete illustration, the two parameter sets below yield the same signal-to-noise for all modules, but parameter set 2 will have a longer (and presumably better) 4-step phase cycle.

	Parameter set 1, NS=2	Parameter set 2, NS=4
cnst51	12	6
cnst52	8	4
cnst53	2	1
cnst51 − cnst52 − cnst53	2	1

The parameter `NBL` should still be set to 2 for all of the supersequences shown in this work. The `NBL` parameter corresponds to the number of *horizontally* concatenated modules, which in all cases is only 2; interleaved modules play no role here. The value of `TD1` should then be set to `cnst51` × `NBL` × N_1, where N_1 is the desired number of t_1 increments (i.e. `TD1` in a 'traditional' 2D experiment).

Finally, it should be noted that the `if/else` conditionals are evaluated only at runtime by the spectrometer. TopSpin does not calculate ahead of time when each interleaved module is run. This means that the TopSpin `expt` command (which shows the expected experimental duration) can yield (very slightly) erroneous results.

S2 NOAH-4 AB$_N$NS experiment

Since the ^{1}H–^{1}H NOESY uses the same ^{1}H$^{!C}$ magnetisation as ^{13}C HMBC so can be directly substituted in its place, leading to a NOAH-4 AB$_N$NS supersequence (Figure S2). This not only provides a wealth of through-bond correlations which aid in eludicating molecular constitution, but also furnishes through-space correlations for the determination of configuration or conformation.

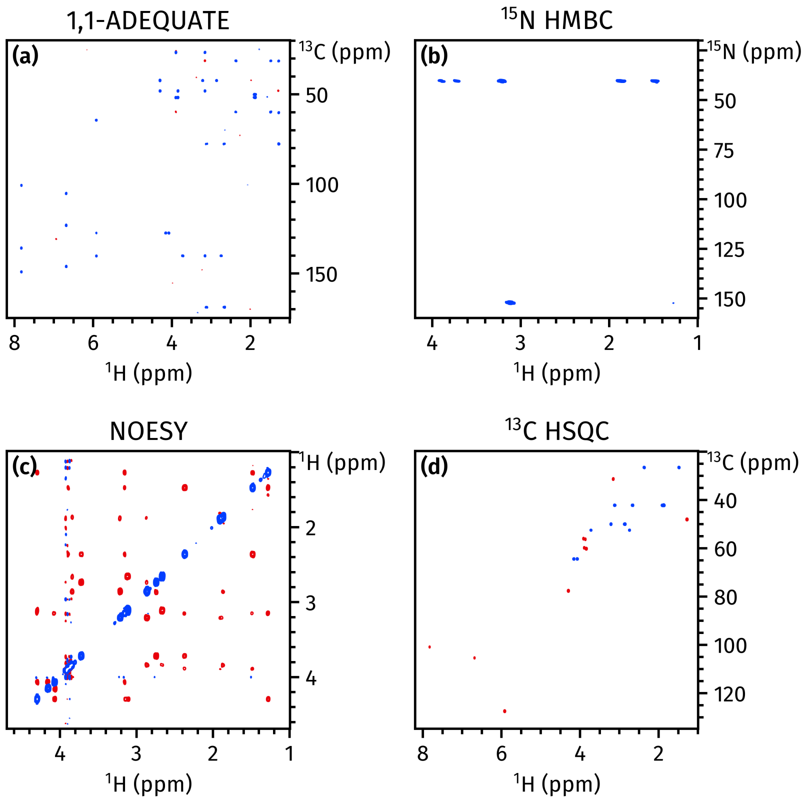

Figure S2: Spectra obtained from the NOAH-4 AB$_N$NS supersequence. **(a)** 1,1-ADEQUATE (16 transients). **(b)** ^{15}N HMBC (12 transients). **(c)** NOESY (2 transients, 800 ms mixing time). **(d)** ^{13}C HSQC (2 transients). Spectra were obtained on a 700 MHz Bruker AV III equipped with a TCI H/C/N cryoprobe; the sample used was 50 mM brucine in CDCl$_3$.

S3 ABBS comparison with and without DIPSI

As described in the main text, the NOAH-4 AB_NBS supersequence is implemented with an extra DIPSI-2 mixing period (of 35 ms) between the ADEQUATE and HSQC modules. The aim of this is to redistribute $^{1}H^{!C}$ magnetisation to ^{13}C-bound protons, thus increasing the sensitivity of the HSQC experiment. Figure S3 compares the results obtained with and without this DIPSI block.

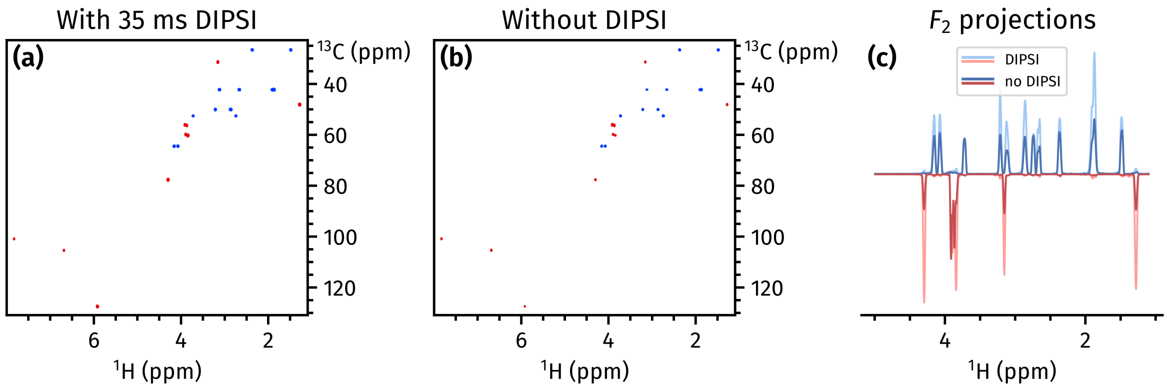

Figure S3: ^{13}C HSQC spectra obtained from the NOAH-4 AB_NBS experiment (Figure 1d). **(b)** With 35 ms DIPSI mixing between the ADEQUATE and ^{13}C HSQC modules (this spectrum is the same as in Figure 4d). **(a)** Without DIPSI mixing between the ADEQUATE and ^{13}C HSQC modules. **(c)** Projections of the spectra in (a) and (b) onto the F_2 axis. Spectra were obtained on a 700 MHz Bruker AV III equipped with a TCI H/C/N cryoprobe; the sample used was 50 mM brucine in $CDCl_3$.

The spectral quality in both cases is acceptable. However, the spectrum acquired with DIPSI mixing (Figure S3b) is weaker, which is more clearly shown in the projections onto the F_2 axes (Figure S3c). When DIPSI mixing is added, the average signal enhancement across all peaks in the HSQC is 88% (Figure S3). These observations are consistent with previous studies on NOAH supersequences containing two successive $^{1}H^{C}$ modules.[1]

S4 Cyclosporin structure

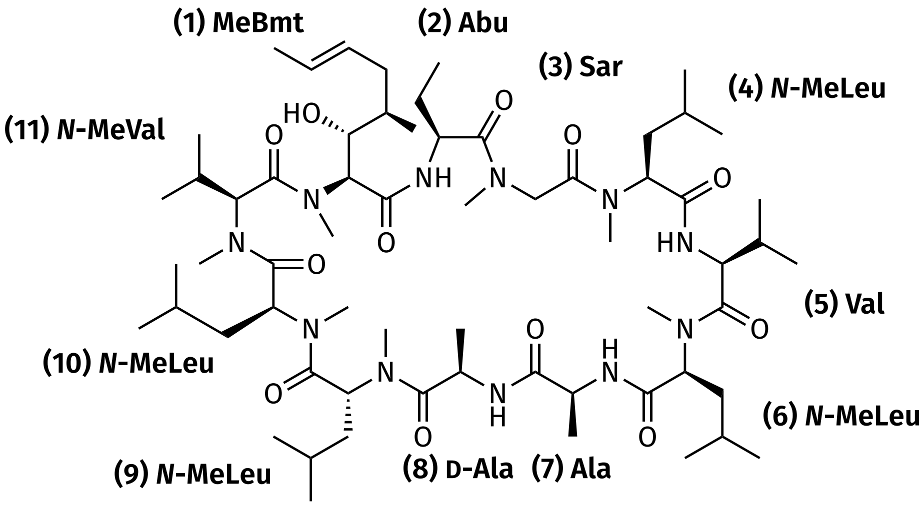

Figure S4: Structure of cyclosporin with residues numbered.

The residue numbers shown here correspond to the labelling of the peaks in Figures 6b and 6c.

S5 Symmetrisation procedure

In Figure 6c, the ^{13}C–^{13}C one-bond covariance spectrum has been subjected to a sign-preserving symmetrisation procedure. This is defined by replacing the intensity at each point $p(\Omega_1, \Omega_2)$ by

$$p(\Omega_1, \Omega_2) \rightarrow \mathrm{sgn}[p(\Omega_1, \Omega_2)] \cdot \min\{|p(\Omega_1, \Omega_2)|, |p(\Omega_2, \Omega_1)|\}\,. \tag{1}$$

Here, sgn p refers to the sign of p, or equivalently $p/|p|$ (for $p \neq 0$). The sgn p term ensures that the *sign* of each peak (and hence multiplicity information) is preserved, but the (absolute) intensities are symmetrised about the main diagonal, which suppresses artefactual responses arising from coincidental peak overlap.

It should be noted that such a procedure can only be safely carried out where peaks on both sides of the diagonals are expected to be seen. For a *true* ^{13}C–^{13}C correlation spectrum, this would be the case for all pairs of ^{13}C nuclei. However, the covariance spectrum shown in Figures 6b and 6cdoes not satisfy this: peaks at (Ω_1, Ω_2) are only observed if the carbon at Ω_2 is bonded to at least one proton. Thus, if the symmetrisation procedure is applied across the entire spectrum, correlations between quaternary and non-quaternary carbons (such as those in Figure 6b) will be lost. However, in the case of Figure 6c, the alkyl region of cyclosporin does not contain any quaternary carbons, allowing the symmetrisation can be safely carried out.

References

(1) Yong, J. R. J.; Hansen, A. L.; Kupče, Ē.; Claridge, T. D. W. Increasing sensitivity and versatility in NMR supersequences with new HSQC-based modules. *J. Magn. Reson.* **2021**, *329*, 107027, DOI: 10.1016/j.jmr.2021.107027.